15. V. K. Gribkoff *et al.*, *Mol. Pharmacol.* **50**, 206 (1996).
16. T. Miura, Y. Liu, H. Kita, T. Ogawa, K. Shimamoto, *J. Am. Coll. Cardiol.* **35**, 238 (2000).
17. G. A. Kimmich, H. Rasmussen, *Biochim. Biophys. Acta* **131**, 413 (1967).
18. A. P. Halestrap, *Biochim. Biophys. Acta* **973**, 355 (1989).
19. A. J. Kowaltowski, S. Seetharaman, P. Paucek, K. D. Garlid, *Am. J. Physiol. Heart Circ. Physiol.* **280**, H649 (2001).
20. M. Murata, M. Akao, B. O'Rourke, E. Marban, *Circ. Res.* **89**, 891 (2001).
21. L. Wang *et al.*, *Am. J. Physiol. Heart Circ. Physiol.* **280**, H2321 (2001).
22. Z. Yao *et al.*, *Am. J. Physiol. Heart Circ. Physiol.* **277**, H2504 (1999).
23. R. A. Forbes, C. Steenbergen, E. Murphy, *Circ. Res.* **88**, 802 (2001).
24. T. Pain *et al.*, *Circ. Res.* **87**, 460 (2000).
25. T. Grimmsmann, I. Rustenbeck, *Br. J. Pharmacol.* **123**, 781 (1998).
26. R. G. Hansford, A. L. Lehninger, *Biochem. J.* **126**, 689 (1972).
27. R. Paliwal, G. Costa, J. J. Diwan, *Biochemistry* **31**, 2223(1992).
28. J. J. Diwan, T. Haley, D. R. Sanadi, *Biochem. Biophys. Res. Commun.* **153**, 224(1988).
29. P. Paucek *et al.*, *J. Biol. Chem.* **267**, 26062 (1992).
30. D. Siemen, C. Loupatatzis, J. Borecky, E. Gulbins, F. Lang, *Biochem. Biophys. Res. Commun.* **257**, 549 (999).
31. Supported by NIHR01HL54598 (B.O'R.) and CIHR 49843 (J.V.E.). We thank P. L. Pedersen and Y. H. Ko for the liver submitochondrial particles and M. Aon and E. Marbán for helpful comments.

Supporting Online Material
www.sciencemag.org/cgi/content/full/298/5595/1029/DC1.
Materials and Methods

24 May 2002; accepted 12 September 2002

Hijacking of Host Cell IKK Signalosomes by the Transforming Parasite *Theileria*

Volker T. Heussler,[1]*† Sven Rottenberg,[1]* Rebekka Schwab,[1] Peter Küenzi,[1] Paula C. Fernandez,[1] Susan McKellar,[2] Brian Shiels,[2] Zhijian J. Chen,[3] Kim Orth,[3] David Wallach,[4] Dirk A. E. Dobbelaere[1]‡

Parasites have evolved a plethora of mechanisms to ensure their propagation and evade antagonistic host responses. The intracellular protozoan parasite *Theileria* is the only eukaryote known to induce uncontrolled host cell proliferation. Survival of *Theileria*-transformed leukocytes depends strictly on constitutive nuclear factor kappa B (NF-κB) activity. We found that this was mediated by recruitment of the multisubunit IκB kinase (IKK) into large, activated foci on the parasite surface. IKK signalosome assembly was specific for the transforming schizont stage of the parasite and was down-regulated upon differentiation into the nontransforming merozoite stage. Our findings provide insights into IKK activation and how pathogens subvert host-cell signaling pathways.

Theileria parva and *Theileria annulata* are tick-transmitted protozoan parasites of cattle that cause severe lymphoproliferative diseases in large areas of Africa and Asia. Unprotected animals that become infected almost invariably succumb to theileriosis. *Theileria* spp. are closely related to other apicomplexan parasites, such as *Plasmodium*, *Toxoplasma*, and *Babesia* spp. The intracellular schizont stages of *T. parva* and *T. annulata* possess the capacity to transform the target host cells they infect. *T. parva* transforms T cells or B cells, whereas *T. annulata* induces uncontrolled proliferation of cells of monocyte/macrophage lineage and B cells. The pronounced pathology and mortality caused by *Theileria* infections is tightly associated with the parasite's transforming capacity. *Theileria*-transformed cells acquire a metastatic phenotype, allowing them to proliferate in nonlymphoid as well as lymphoid host tissues, and also to form tumors when injected into immunocompromised mice (*1*).

Among its many functions, the transcription factor NF-κB also contributes to the regulation of genes that prevent apoptosis (*2*). Stimuli that trigger NF-κB activation all converge onto a multisubunit kinase complex called IKK (IκB kinase) that consists of two catalytic subunits, IKK1 (IKKα) and IKK2 (IKKβ), and a modulating subunit NEMO (IKKγ). IKK phosphorylates IκBs, the cytoplasmic inhibitors of NF-κB, tagging them for proteasomal degradation, thus allowing NF-κB to translocate to the nucleus (*3*). In *Theileria*-transformed cells, NF-κB is constitutively activated in a parasite-dependent manner (*4*, *5*). This results in the expression of a number of κB-dependent genes, including several anti-apoptotic genes such as c-*FLIP*, c-*iap*, and *xiap* (*6*). Interference with the NF-κB pathway in *Theileria*-transformed cells results in rapid apoptosis (*7*). Although the biological relevance of constitutive NF-κB activity in the survival of *Theileria*-transformed leukocytes is obvious, the way in which the parasite induces NF-κB activation is still unknown.

In contrast to most other apicomplexan parasites, which are enclosed in parasitophorous vacuoles, *Theileria* schizonts inhabit the host cell cytoplasm (*8*), where they are exposed to the cytosol and cytoskeleton of the infected cell. Several drugs, described in other systems to interfere with upstream components of the NF-κB activation cascade, fail to block *Theileria*-induced NF-κB activity (*9*), suggesting that the parasite might short-circuit the NF-κB activation pathway. We performed dual-staining confocal immunofluorescence microscopy using antibodies directed against a parasite surface protein, PIM, in combination with antibodies directed against subunits of the IKK complex (Fig. 1). Surprisingly, we found the *T. parva* schizont to be decorated with macromolecular foci detected by antibodies to IKK1 (Fig. 1A), IKK2, and NEMO (fig. S1). The number of IKK foci clustered at the parasite surface correlated with the size of the schizont, which can differ considerably from cell to cell. In addition, the size of the foci varied from structures that were barely detectable by light microscopy to particles with an apparent diameter of several hundred nanometers. V5-epitope–tagged forms of bovine IKK1, IKK2, or NEMO expressed in *T. parva*–transformed T cells became incorporated into the parasite-associated foci (shown for IKK2 in Fig. 1B), demonstrating that the foci can accommodate the different bovine IKK components. IKK foci could also be detected in *T. parva*–transformed B cells, as well as in monocyte/macrophage-derived cell lines and B cell lines transformed by *T. annulata* (Fig. 2).

The IKK complex is often referred to as the "IKK signalosome" because of its size (*10*), but activated signalosomes have not been visualized so far. Using in vitro kinase assays, we detected robust IKK activity in *T. parva*–transformed T cells (*11*). More importantly, phospho-specific antibodies readily detected phosphorylated forms of IKK (P-

[1]Division of Molecular Pathology, Institute of Animal Pathology, University of Bern, CH-3012 Bern, Switzerland. [2]Department of Veterinary Parasitology, University of Glasgow, Glasgow G61-1QH Scotland. [3]Department of Molecular Biology, University of Texas Southwestern Medical Center, Dallas, TX 75390–9148, USA. [4]Department of Biological Chemistry, Weizmann Institute of Science, Rehovot, 76100, Israel.

*These authors contributed equally to this work.
†Present address: Berhard-Nocht-Institute for Tropical Medicine, D-20359 Hamburg, Germany.
‡To whom correspondence should be addressed: E-mail: dirk.dobbelaere@itpa.unibe.ch

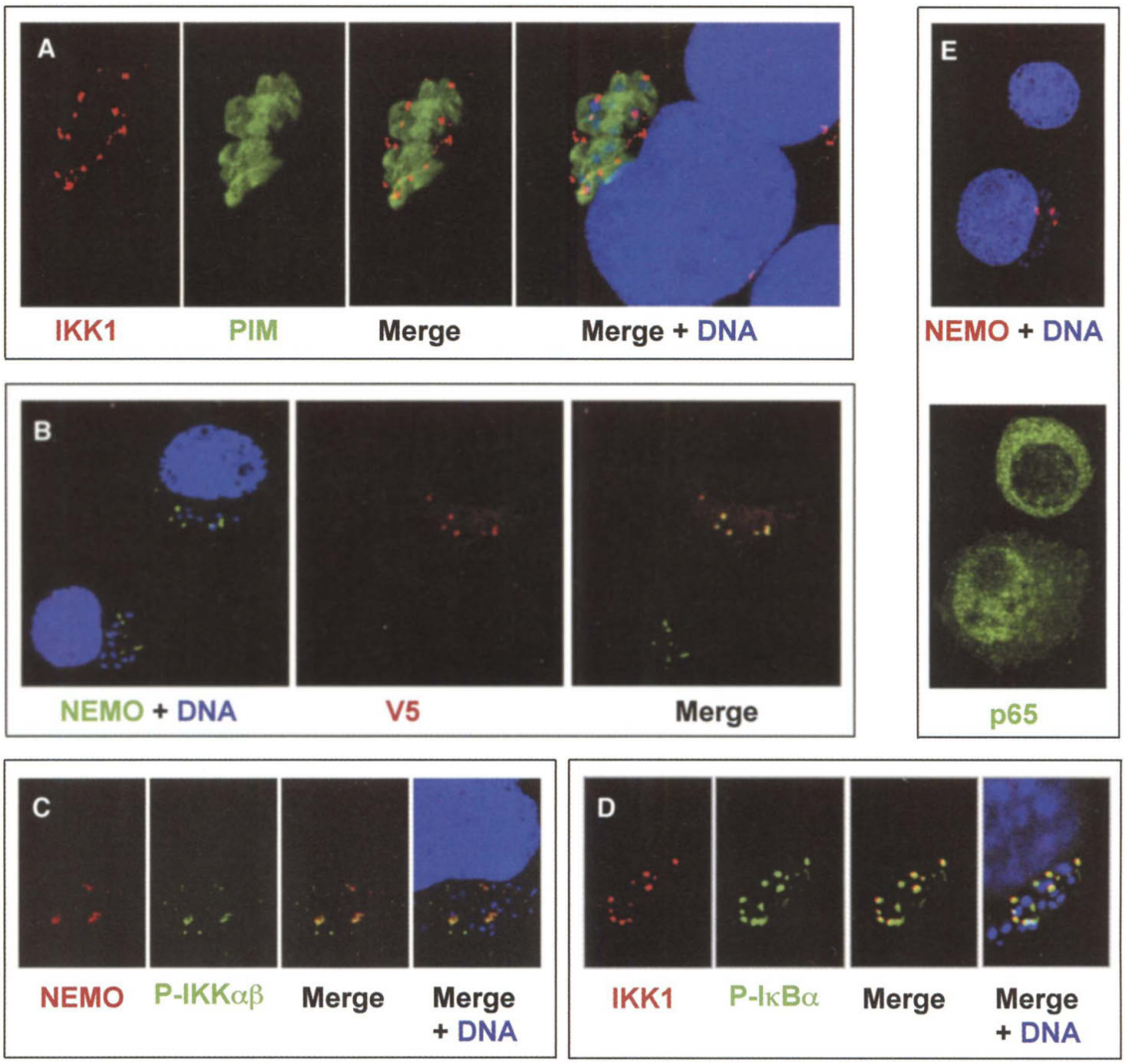

Fig. 1. Activated IKK signalosomes associate with the intracellular parasite *Theileria*. Confocal immunofluorescence microscopy analysis of *T. parva*–transformed T cells. (**A**) Anti-IKK1 reveals the assembly of IKK foci (red) at the surface of the *Theileria* schizont (detected by anti-PIM, green). "Merge" represents an overlay of the two images. "DNA" indicates staining of host cell and parasite nuclei with Hoechst DNA Dye. (**B**) V5-epitope–tagged IKK2 (red) colocalizes with parasite-associated IKK foci detected by anti-NEMO (green). Colocalization, indicated by the appearance of a yellow color (merge), is only observed in the transfected (upper) cell. (**C**) Parasite-associated IKK foci (NEMO, red) are specifically phosphorylated (P-IKKαβ, green), reflecting activation. (**D**) Activated IKK signalosomes (IKK1, red) also contain phosphorylated IκBα (P-IκBα, green). (**E**) IKK signalosomes (NEMO, red) cannot be detected in cells that do not harbor the parasite (parasite nuclei are absent in the upper cell). The presence of parasite-associated IKK signalosomes correlates with the nuclear presence of NF-κB (detected by anti-p65, green).

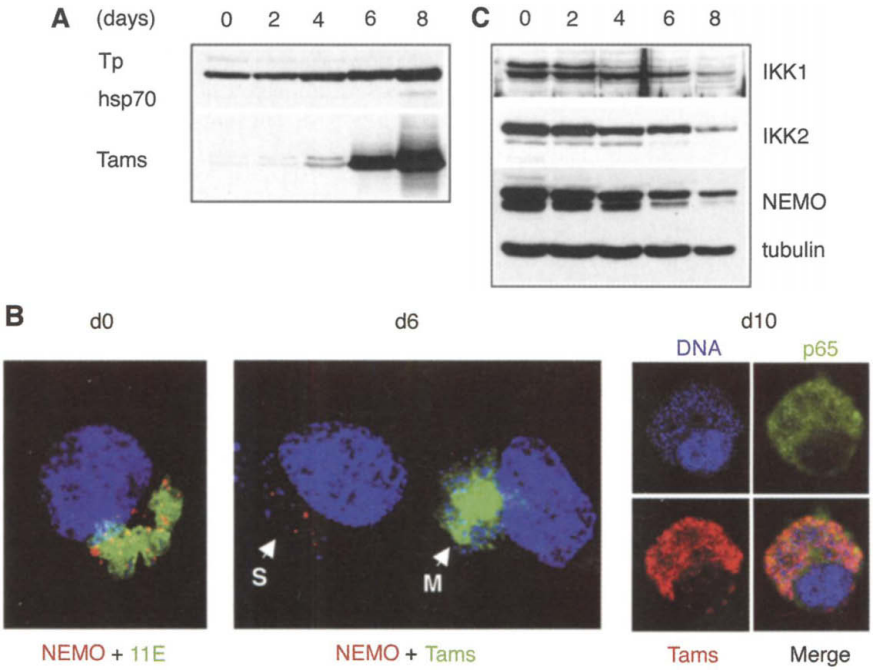

Fig. 2. The assembly of parasite-associated IKK signalosomes is specific for the transforming schizont stage of the parasite. (**A**) *T. annulata*–transformed cells were exposed to heat shock (41°C) for 8 to 10 days to induce differentiation to the merozoite stage of the life cycle. Immunoblot analysis shows that this is accompanied by a gradual increase in hsp70 expression and the strong induction of the merozoite-specific surface antigen Tams1. (**B**) Confocal immunofluorescence analysis showing the association of IKK signalosomes (detected by anti-NEMO, red) with the *T. annulata* schizont (detected by an antibody directed against the schizont protein 11E, green) in cells cultured at 37°C (d0, left). Schizonts that are still present after 6 days of heat shock (labeled "S", d6, middle) are still decorated with IKK signalosomes (NEMO, red), whereas parasites undergoing merogony ("M"; labeled with anti-Tams1, green) are not. After 10 days of heat shock (d10), the cells contain almost exclusively merozoites (multiple parasite nuclei stained by Hoechst DNA dye, blue) that are detectable by anti-Tams1 (red); in such cells, staining with anti-p65 (green) reveals that NF-κB is cytoplasmic and is not detectable in the host cell nucleus. "Merge" represents an overlay of the different staining patterns for the same cell, showing the presence of merozoites and NF-κB in the cytoplasm (yellow-orange), and the host and parasite nuclei stained blue. (**C**) In cells harboring differentiating parasites, the reduction in the levels of IKK1, IKK2, and NEMO is more pronounced than that of host cell tubulin.

IKK) and its substrate IκBα (P-IκBα) in parasite-associated foci (Fig. 1, C and D), demonstrating that these represent activated IKK signalosomes. Because IκBα is constantly being phosphorylated, degraded, and expressed de novo in *T. parva*–infected cells (*5*), the P-IκBα observed in IKK signalosomes most likely reflects the steady-state pool of phosphorylated IκBα.

Occasionally (<5%) the schizont is not partitioned between daughter cells during mitosis, and cells without the parasite cease to proliferate and eventually undergo apoptosis (*1*). IKK signalosomes were not seen in cells that did not contain schizonts, and NF-κB was also absent from the nucleus of these cells (Fig. 1E). The transformed phenotype of *Theileria*-infected leukocytes and accompanying persistent NF-κB activity depend on the continuous presence of the parasite and can be reversed by treating cells with the theilericidal compound BW720c (*1*). The drug interferes specifically with the parasite's electron transport chain, inducing parasite death and elimination from the host cell (*12*). This was reflected by the gradual disappearance of parasite proteins from cell lysates (fig. S2). Cells cured of the parasite ceased to proliferate within 3 to 5 days (*13*), and microscopically visible IKK complexes disappeared over 24 to 48 hours (fig. S1). This coincided with decreased translocation of NF-κB to the host cell nucleus (fig. S3). Levels of NEMO and IKK remained largely constant, suggesting a redistribution of IKK proteins in the cell rather than a process of active degradation (fig. S2).

Proliferation of *Theileria*-transformed cells is tightly linked to the schizont stage of the parasite. In the *T. annulata*–transformed cell line D7, heat-induced differentiation of schizonts to merozoites (the erythrocyte-infective stages of the parasite) is accompanied by the expression of the merozoite surface antigen Tams1 (Fig. 2A) and gradual loss of the transformed phenotype (*14*). As merogony progressed over a period of 8 to 10 days, host cells ceased to proliferate, and parasite-associated IKK signalosomes decreased steadily (Fig. 2B). In cells containing merozoites, nuclear staining with anti-p65 was also low. This process was accompanied by a marked reduction in the levels of IKK proteins (Fig. 2C) coincident with an increase in the parasite protein Tams1.

During immunofluorescence analysis, we noticed that the number of parasite-associated IKK signalosomes fluctuated in the course of the host cell cycle. In cells in metaphase, anaphase, or telophase, few IKK signalosomes were seen as compared to cells in interphase or early prophase. Furthermore, parasite-associated IKK foci were detected in only 4.3% of cells arrested in mitosis by colchicine treatment, as compared to 64% for interphase cells (fig. S4). IKK signalosomes were associated with the parasite throughout host cell interphase, irrespective of whether cells were in S phase or G_1/G_2.

IKK activation pathways triggered by pro-inflammatory mediators, such as tumor necrosis factor–α (TNF-α), interleukin-1 (IL-1), and lipopolysaccharides, have been shown to involve common upstream adaptor proteins such as TRAF2 or TRAF6, as well as a range of kinases and regulatory molecules (*3*, *15*). To determine whether upstream components participate in parasite-induced NF-κB activation, we overexpressed dominant-negative mutant forms of these molecules and monitored κB-dependent reporter gene expression. Overexpression of dominant-negative mutant forms of TRAF6 and TRAF2, the ubiquitin conjugase Ubc13, or RIP did not interfere with NF-κB–dependent reporter gene expression, nor did the negative regulator A20 (*16*) (Fig. 3A). Wild-type or mutant forms of POSH (*17*), an SH3-containing scaffold protein and target of Rac, also failed to block parasite-induced NF-κB transcriptional activity. In addition, catalytically inactive forms of the IKK kinases MEKK1, NAK, and TAK all failed to block constitutive NF-κB activity (*11*). Kinase-defective NIK has been shown to block NF-κB activation induced through several pathways, but its precise role is still enigmatic (*3*, *15*). NIK is probably not an essential component in *T. parva*–induced constitutive NF-κB activation, because overexpression of kinase-defective NIK reduced luciferase reporter gene activity by only 25% (*11*). In addition, the phosphatidylinositol 3-kinase/protein kinase B pathway, although constitutively active in *Theileria*-transformed leukocytes, is not involved in parasite-induced NF-κB activation (*18*). Importantly, RIP2 (also called RICK, CCK, or CARDIAC) (*19*), a kinase with an important function in innate and adaptive immunity (*20*, *21*) and NF-κB activation in response to intracellular bacteria (*22*), did not contribute to *Theileria*-induced NF-κB activation (Fig. 3B).

In contrast, interference at the level of the IKK signalosome itself blocked parasite-induced NF-κB activity (Fig. 3B). Overexpressing kinase-inactive IKK2, but not IKK1, inhibited NF-κB transcriptional activity by ~50%. As has been reported in other systems (*23*, *24*), overexpression of both wild-type and COOH-terminally–truncated NEMO also resulted in reduced NF-κB–dependent reporter gene expression. Moreover, YopJ, an IKK2-binding protein secreted by *Yersinia pestis* (*25*), was capable of overriding *Theileria*-induced NF-κB activation, whereas the catalytically inactive mutant YopJ-C172A did not inhibit NF-κB activation. The strongest inhibition (up to 80%), however, was obtained by overexpressing $I\kappa B^{S32A}$, a degradation-resistant repressor form of IκBα (Fig. 3B) (*7*). Incubation of *T. parva*–transformed T cells with a cell-permeable inhibitor peptide (NBD-peptide) corresponding to the NEMO-binding domain of IKK

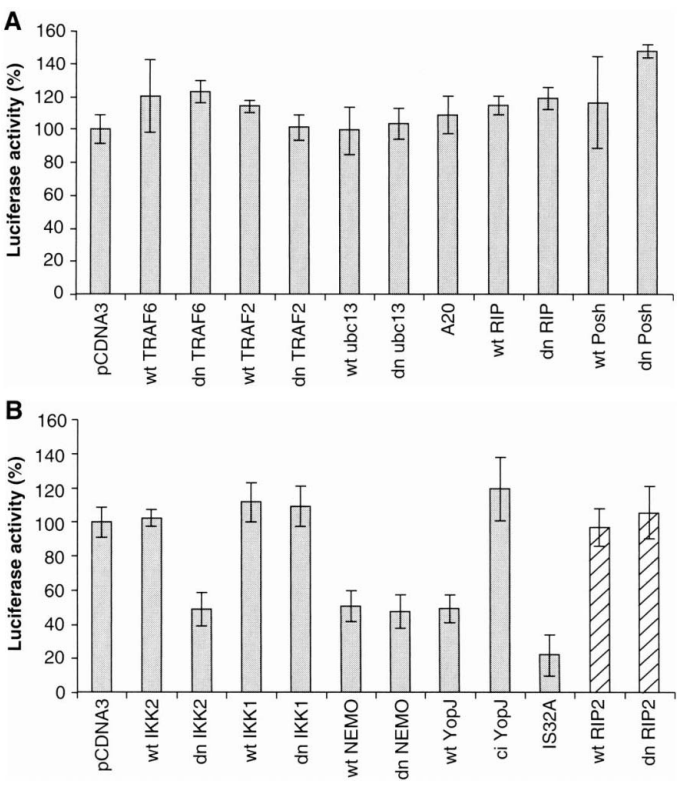

Fig. 3. Interference with NF-κB activation pathways upstream of IKK does not affect parasite-induced NF-κB activation; blocking at the level of the IKK complex does. **(A)** Relative luciferase activity (%) measured in *T. parva*–transformed cells cotransfected with a κB-dependent luciferase reporter construct and plasmids encoding either wild-type (wt) or dominant-negative mutant (dn) forms of different components of the NF-κB pathway that function upstream of IKK. **(B)** Cells were cotransfected with wt or dn forms of the different IKK components, with wt or catalytically inactive (ci) YopJ, or with a mutant form of IκBα (I^{S32A}) that cannot be degraded. Hatched bars represent relative NF-κB–dependent luciferase activity in cells transfected with constructs expressing wt or dn mutant forms of RIP2. In control experiments, all constructs were capable of blocking classic NF-κB activation pathways in uninfected bovine leukocytes (fig. S5).

(*26*), but not with the control peptide, reduced the number of parasite-associated IKK signalosomes containing P-IκBα by 83%. These data confirm a role for NEMO in parasite-associated IKK signalosome activation. Taken together, our observations strongly indicate that the parasite bypasses the common upstream adaptor proteins and kinases that link surface receptor stimulation to IKK activation. This mechanism is compatible with a model called "proximity-induced activation," in which the enforced oligomerization of IKK components or adaptor proteins suffices to induce NF-κB activation (*3*, *15*, *27–29*).

Despite extensive efforts, a direct association between parasite proteins and IKK could not be demonstrated. The focal pattern of IKK association with the parasite, together with the cell cycle–dependent appearance of activated IKK signalosomes, suggests that host cell molecules other than IKK may participate in the interaction.

Pathogen-derived products have been shown to interact directly with host cell signaling pathways at different levels. *Theileria* perverts the NF-κB pathway through an unusual mechanism involving the aggregation of critical pathway components at the surface of the transforming schizont stage. In contrast, the merozoite no longer requires host cell survival and ceases to activate the NF-κB pathway. Parasite-induced NF-κB activity is clearly crucial for the survival—and potentially also the proliferation—of *Theileria*-transformed cells (*7*). It can also be predicted, however, that NF-κB–dependent activation of inflammatory genes will contribute to the pathogenesis of theileriosis.

References and Notes

1. Reviewed in D. Dobbelaere, V. Heussler, *Annu. Rev. Microbiol.* **53**, 1 (1999).
2. M. Karin, A. Lin, *Nature Immunol.* **3**, 221 (2002).
3. Reviewed in S. Ghosh, M. Karin, *Cell* **109** (suppl.), S81 (2002).
4. V. Ivanov *et al.*, *Mol. Cell. Biol.* **9**, 4677 (1989).
5. G. H. Palmer *et al.*, *Proc. Natl. Acad. Sci. U.S.A.* **94**, 12527 (1997).
6. P. Küenzi, D. Dobbelaere, unpublished data.
7. V. T. Heussler *et al.*, *Proc. Natl. Acad. Sci. U.S.A.* **96**, 7312 (1999).
8. M. K. Shaw, *Int. J. Parasitol.* **27**, 457 (1997).
9. J. Machado, P. C. Fernandez, I. Baumann, D. A. Dobbelaere, *Microbes Infect.* **2**, 1311 (2000).
10. F. Mercurio *et al.*, *Science* **278**, 860 (1997).
11. V. T. Heussler *et al.*, data not shown.
12. A. T. Hudson *et al.*, *Parasitology* **90**, 45 (1985).
13. D. A. Dobbelaere, T. M. Coquerelle, I. J. Roditi, M. Eichhorn, R. O. Williams, *Proc. Natl. Acad. Sci. U.S.A.* **85**, 4730 (1988).
14. B. Shiels *et al.*, *J. Cell Sci.* **101**, 99 (1992).
15. Reviewed in M. Karin, M. Delhase, *Semin. Immunol.* **12**, 85 (2000).
16. H. Y. Song, M. Rothe, D. V. Goeddel, *Proc. Natl. Acad. Sci. U.S.A.* **93**, 6721 (1996).
17. N. Tapon, K. Nagata, N. Lamarche, A. Hall, *EMBO J.* **17**, 1395 (1998).
18. V. T. Heussler *et al.*, *Cell. Microbiol.* **3**, 537 (2001).
19. J. V. McCarthy, J. Ni, V. M. Dixit, *J. Biol. Chem.* **273**, 16968 (1998).
20. A. I. Chin *et al.*, *Nature* **416**, 190 (2002).
21. K. Kobayashi *et al.*, *Nature* **416**, 194 (2002).
22. S. E. Girardin *et al.*, *EMBO Rep.* **19**, 19 (2001).
23. S. Q. Zhang, A. Kovalenko, G. Cantarella, D. Wallach, *Immunity* **12**, 301 (2000).
24. D. Krappmann *et al.*, *J. Biol. Chem.* **275**, 29779 (2000).
25. K. Orth *et al.*, *Science* **285**, 1920 (1999).
26. M. J. May *et al.*, *Science* **289**, 1550 (2000).
27. V. Baud *et al.*, *Genes Dev.* **13**, 1297 (1999).
28. N. Inohara *et al.*, *J. Biol. Chem.* **275**, 27823 (2000).
29. J. L. Poyet *et al.*, *J. Biol. Chem.* **275**, 37966 (2000).

30. We thank I. Roditi for critical reading of the manuscript. We also thank S. Grimm for technical assistance; D. Werling and T. Jungi for lipopolysaccharide, bovine TNF-α, and IL-1; L. Schmitz for recombinant IκBα; A. Hall for the POSH constructs; R. Toftgård for the TRAF-2 constructs, and J. Naessens for anti-PIM. This research was supported by grants 31-61340.00 (D.A.E.D.) and 31.44407.95 (P.C.F.) from the Swiss National Science Foundation, grant KFS-00625-2-1998 from Krebsforschung Schweiz, and by the INCO/TANVAC project (Federal Office for Education and Science, BBW 01.0093). B.S. was supported by Wellcome Trust grant 58933, Z.J.C. by grants from the National Institute of Health (GM63692) and the Robert A. Welch Foundation, K.O. by the Endowed Scholars Program at the University of Texas Southwestern Medical Center, D.W. by grants from Inter-Lab, Ltd., and Ness Ziona (Israel) and Ares Trading S.A. (Switzerland).

Supporting Online Material

www.sciencemag.org/cgi/content/full/298/5595/1033/DC1
Materials and Methods
Figs. S1 to S5
References

26 June 2002; accepted 12 September 2002

RNA Polymerase II Transcription in Murine Cells Lacking the TATA Binding Protein

Igor Martianov, Stephane Viville, Irwin Davidson*

Inactivation of the murine TATA binding protein (TBP) gene by homologous recombination leads to growth arrest and apoptosis at the embryonic blastocyst stage. However, after loss of TBP, RNA polymerase II (pol II) remains in a transcriptionally active phosphorylation state, and in situ run-on experiments showed high levels of pol II transcription comparable to those of wild-type cells. In contrast, pol I and pol III transcription was arrested. Our results show a differential dependency of the RNA polymerases on TBP and provide evidence for TBP-independent pol II transcriptional mechanisms that allow reinitiation and maintenance of gene transcription in vivo.

In vertebrates, TBP and the TBP-like factor (TLF, also called TBP-related factor 2 or TRF2) are two closely related proteins involved in RNA pol II transcription (*1*). Both proteins share an evolutionarily conserved saddle-like core domain responsible for DNA binding and interaction with the general transcription factors. TBP is a subunit of the pol II transcription factor TFIID and is thought to play a general role in pol II transcription as well as in pol I and pol III transcription (*2*).

In the African clawed toad *Xenopus laevis* and the zebrafish *Danio rerio*, both TBP and TLF are involved in gene expression at the onset of zygotic pol II transcription and during subsequent embryonic development (*3*, *4*). In contrast, murine TLF is neither expressed (fig. S1) nor required (*5*) during early embryogenesis, whereas murine TBP is expressed at all stages.

The gene encoding murine TBP was inactivated by homologous recombination after insertion of the hygromycin resistance gene into exon III (*6*) (fig. S2A). Embryonic stem cell clones bearing the inactivated allele were identified by Southern blot analysis, and $TBP^{+/-}$ mice (fig. S2B) were generated. $TBP^{+/-}$ mice were born at Mendelian frequency, were of normal size and weight, displayed no obvious abnormalities, and were fertile (*7*).

Crossing $TBP^{+/-}$ mice failed to generate viable newborn $TBP^{-/-}$ mice (fig. S2B). However, at day 3.5 postcoitum (E3.5), an approximately Mendelian ratio of $TBP^{-/-}$ blastocysts could be detected with a polymerase chain reaction (PCR) strategy (Fig. 1A). When examined by immunofluorescence for expression of the TBP protein, blastocysts were detected that were totally negative for TBP labeling (Fig. 1B, upper and middle panels). TBP was absent in explanted blastocysts grown for 1 day in vitro (Fig. 1C). Strongly reduced TBP levels were also detected at E2.5 in 8-cell-stage embryos (Fig. 1D), which indicates that the maternal TBP pool was significantly depleted at this stage and was undetectable by the blastocyst stage.

Blastocysts from $TBP^{+/-}$ crosses were explanted at E3.5 (day 0) and cultivated in vitro (*6*). Approximately 25% of the blastocysts

Institut de Génétique et de Biologie Moléculaire et Cellulaire (IGBMC), CNRS/INSERM/ULP, B.P. 163, 67404 Illkirch Cédex, Communauté Urbaine de Strasbourg, France

*To whom correspondence should be addressed. E-mail: irwin@titus.u-strasbg.fr